

Comparison between Tokamak and Ohmically Heated Stellarator Plasmas

D. W. Atkinson, A. N. Dellis, R. D. Gill, D. J. Lees, W. Millar, B. A. Powell,
P. A. Shatford, and D. R. A. Webb

EURATOM—United Kingdom Atomic Energy Authority Fusion Association, Culham Laboratory, Abingdon,
Oxon, OX14 3DB, England

(Received 2 September 1976)

Tokamak and Ohmically heated stellarator plasmas have been compared in the CLEO apparatus, using gas current in the range 10–25 kA at a toroidal field of 12.7 kG. It is found that the vacuum poloidal field due to the helical winding has a considerable influence on the containment properties. In particular, for the same current the electron energy per unit length is a factor of 2 greater in the stellarator than in the tokamak.

CLEO¹ is a seven-field period, $l=3$ toroidal stellarator with a major radius, R_0 , of 90 cm and a minor radius, r_L , of 13 cm as defined by two circular stainless-steel limiters, fixed inside the 28-cm bore stainless-steel vacuum vessel. The maximum available toroidal field B_ϕ is 20 kG, and the helical winding is designed to carry current I_l up to 120 kA-turns. 25% of the torus inner surface is covered by an active film of titanium before, and if necessary during, the day's run. The base pressure is $\sim 10^{-8}$ Torr.

A tokamak configuration can be set up in this apparatus by not energizing the helical winding, with equilibrium provided by a vertical field. A vertical field is also required for stellarator operation, the typical values at 20-kA externally induced ohmic heating current (I_g) being 70 and 30 G for tokamak and stellarator, respectively. By using Ohmically heated hydrogen plasma with I_g in the range 5–26 kA, a comparison has been made between stellarator and tokamak configurations, most extensively at 17 kA. For the B_ϕ of 12.7 kG and I_l of 61 kA-turns used in this comparison, the separatrix lies outside the limiter. The calculated value of rotational transform for the stellarator vacuum magnetic surface which touches the limiter is $\iota=0.3$. The same value of ι at the plasma edge would be produced in the tokamak mode by an equivalent current I_g of 21 kA.

We have chosen to compare the tokamak with the Ohmically heated stellarator when the plasma edge is determined by the limiter rather than by the separatrix in order to ensure that limiter effects (e.g., recycling) and wall effects are as similar as possible in the two configurations.

The diagnostics used in these experiments were the following: (i) Current and loop voltage measurements. (ii) Position coils. When the vertical field is optimized to produce the longest-lasting tokamak current, these show the current channel to be centered to ± 1 cm. (iii) A single-channel

2-mm microwave interferometer for measurement of \bar{n}_e over a minor diameter. (iv) Photon scattering with a 10-J ruby laser for measurement of $n_e(\bar{r})$, $T_e(r)$. (v) A neutral particle analyzer, using charge exchange, for measurement of \bar{T}_i . (vi) A detector of the absolute intensity of H_α emission, to assess recycling and estimate $\bar{\tau}_n$, the average particle containment time.

Figure 1 shows oscillograms of current, loop voltage, and \bar{n}_e for both tokamak and stellarator, under conditions where the peak gas current \hat{I}_g is 20 kA in each case. The loop voltage is higher for the stellarator. At peak gas current, the values are 4.0 and 6.5 V for tokamak and stellarator, respectively. At peak current, the values of \bar{n}_e for tokamak and stellarator are roughly in the ratio of 1:2.

Measurements of the central value of T_e , $T_e(0)$, and of \bar{n}_e made at peak gas current are shown as a function of \hat{I}_g in Fig. 2 for both tokamak and stellarator over the range 10–26 kA. It is seen that in both cases \bar{n}_e increases linearly with current. The behavior of $T_e(0)$ is rather different for the stellarator. It appears to be essentially

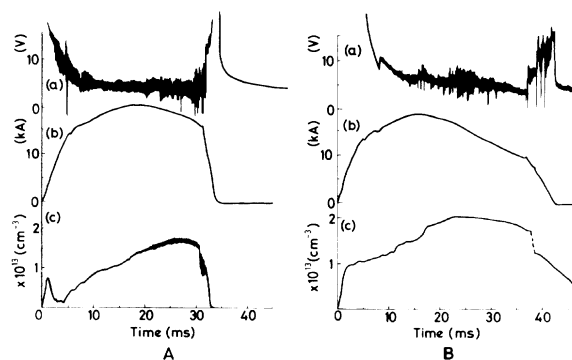


FIG. 1. Oscillograms of (a) loop volts, (b) gas current, (c) mean electron density for (A) tokamak and (B) stellarator at 12.7-kG toroidal field.

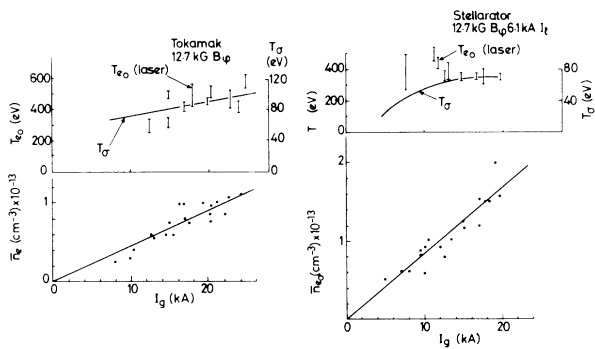


FIG. 2. Central value of T_e and mean density \bar{n}_e as a function of peak gas current for (a) tokamak modes and (b) stellarator modes. Also shown is the conductivity temperature T_σ .

independent of gas current over the range 10–20 kA. The conductivity temperature T_σ , evaluated as a mean, exhibits the same behavior; it increases with current up to 10 kA and then becomes independent of current.

Profiles of $n(r)$ and $T_e(r)$ measured on a vertical plane on one side of the geometric center have been obtained at the peak gas current of 17 kA and toroidal field of 12.7 kG only, for both stellarator and tokamak. These are shown in Fig. 3.

If we infer from these the values of contained electron energy per unit length, W , then they are in the ratio of 2:1 for stellarator and tokamak. This is due solely to the difference in profiles for the two cases, since the central values are approximately the same in each case.

An approximate estimate of $W(I_g)$, obtained by assuming that the profiles do not change with gas current, shows that for both stellarator and tokamak $W \propto I_g(I_g + I_e)$, where $I_e = 0$ for tokamak and

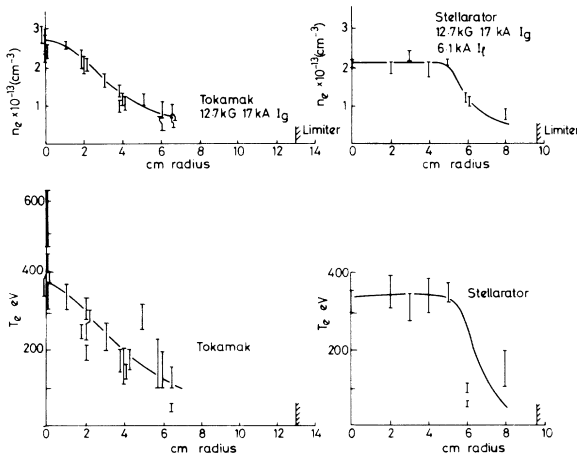


FIG. 3. Radial profiles of n_e and T_e for stellarator and tokamak modes at 12.7-kG B_ϕ and 17-kA I_g .

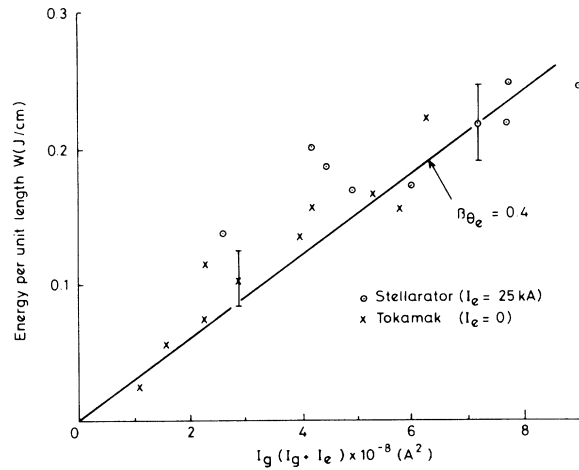


FIG. 4. Electron energy per unit length W , as a function of $I_g(I_g + I_e)$ for stellarator and tokamak modes.

25 kA for stellarator (a value chosen empirically, but close to the theoretical value of 21 kA). This scaling is predicted on the basis of pseudoclassical diffusion and is illustrated in Fig. 4. The full line corresponds to a value of poloidal β for the tokamak [defined as in relation (3) below] of 0.4. These results confirm and extend those of the Uragan I and Wendelstein IIb stellarators.^{2,3}

The dependence of ion temperature on gas current shows an Artsimovich scaling $T_i \propto [(I_g + I_e) \times B_\phi n_e]^{1/3}$. Again there is agreement between stellarator and tokamak if we write $I_e = 25$ kA for the stellarator (Fig. 5).

An overall value of the particle containment time, $\bar{\tau}_n$, was inferred from the absolute H_α emission. The total (time-resolved but space-integrated) emission was measured in each of two

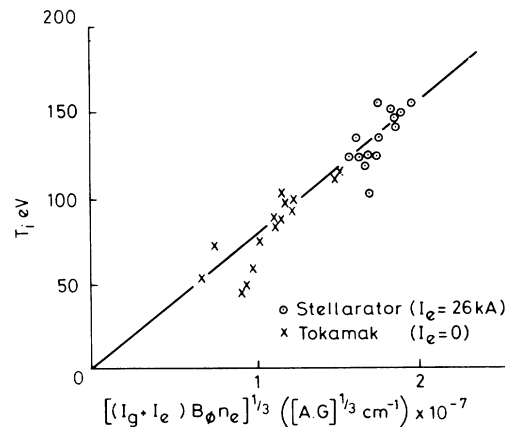


FIG. 5. Ion temperature as a function of $[(I_g + I_e) \times B_\phi n_e]^{1/3}$ for stellarator and tokamak modes.

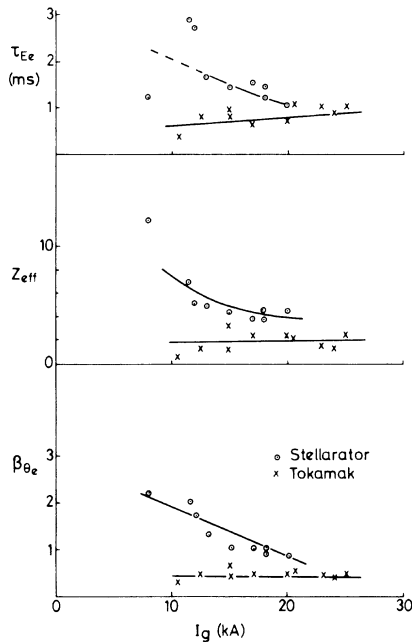


FIG. 6. Energy confinement time, Z_{eff} , and β_{θ_e} as a function of gas current for stellarator and tokamak modes.

narrow sectors, one at 6° and the other at 66° major azimuthal angle from the nearest limiter. Most of the emission came from the vicinity of the limiters, the intensity in the tokamak case being at least twice that in the stellarator. Taking an azimuthal distribution similar to that found for the ST tokamak,⁴ in conjunction with these data, indicates an overall $\bar{\tau}_n$ in the range 4–8 ms for the tokamak and 15–50 ms in the stellarator for the 17-kA gas current condition.

Values of τ_{E_e} , resistance anomaly (Z_{eff}), and β_{θ_e} deduced from the data are shown in Fig. 6. These quantities are defined for our purposes in the following way:

$$\tau_{E_e} = (9.44 \times 10^{-18} R_0 / V I_g) \int_0^a r n T_e dr, \quad (1)$$

$$Z_{eff} = (11.1 V / R_0 I_g) \int_0^a r T_e^{3/2} dr, \quad (2)$$

$$\beta_{\theta_e} = (2.1 \times 10^{-9} / I_g^2) \int_0^a r n T_e dr, \quad (3)$$

(the units are eV, cm, A, and V) where, for the stellarator, the integral is taken over a circle whose area is equal to that of the trefoil-shaped limiting magnetic surface.

As before, we assume that the profiles do not change with gas current and that Z_{eff} is an average over the cross section. It will be seen that Z_{eff} for the tokamak is generally ~ 2 which is reasonable, taking into account the titanium gettering and low power flux to the walls. The value for the

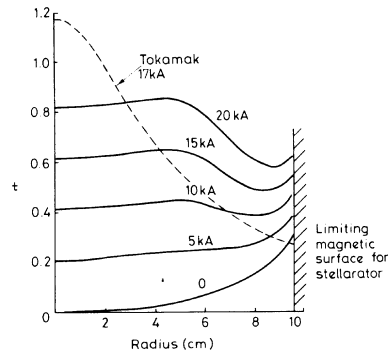


FIG. 7. Total rotational transform as a function of minor radius at the position of the measured temperature profile, for stellarator at 12.7-kG B_ϕ and 61-kA turns I_t , with gas current as a parameter and for tokamak mode at 17-kA I_g .

stellarator is higher, particularly at low gas currents.

These results may be summarized as follows: (i) The stellarator gives an energy confinement time for electrons ≥ 1 ms at 20-kA gas current and $T_e = 350$ eV. (ii) The behavior of the tokamak, in that it gives $\beta_\theta \sim 0.4$ and $\tau_E \sim 1$ msec at $I_g \sim 20$ kA and $B_\phi \sim 13$ kG, is in line with other medium-sized tokamaks, e.g., T3 and ST.^{5,6} It agrees well with the scaling laws proposed by Daughney⁷ and Murakami, Callen, and Berry.⁸ (iii) The confined electron energy is greater in the stellarator than in the tokamak at the same gas current. This is a consequence of the different radial profiles. (iv) The stellarator poloidal vacuum field takes part in plasma containment, as is shown in Fig. 4, in which the contained electron energy varies linearly as $I_g(I_g + I_\theta)$. (v) There is general agreement, over the limited parameter range studied, with pseudoclassical scaling for electron thermal conductivity (Fig. 4) and neoclassical for ion thermal conductivity (Fig. 5), although the value of T_i is about a factor of 2 lower than that given by the well-known Artsimovich formula. This could be associated with the relatively high density of neutrals, $(1-5) \times 10^8 \text{ cm}^{-3}$.⁹ (vi) The profile of $T_e(r)$ may be used to infer a current density profile by assuming that Z_{eff} is constant over the cross section. From this we have plotted Fig. 7 which shows, for the stellarator, the total rotational transform t , as a function of radius at different plasma currents (again assuming the T_e profile to be independent of plasma current). It will be seen that we have a total value of $q_{edge} \approx 1.4$ without any signs of disruption.

A tokamak profile, based on the 17-kA results

is also shown for comparison. The lack of shear in the stellarator should be noted, in contrast to the tokamak case.

The authors would like to thank Dr. R. J. Bickerton for his advice and encouragement during this work.

¹P. Reynolds, P. Millward, and R. R. Hunt, in *Proceedings of the Fifth International Conference Plasma Physics and Controlled Nuclear Fusion Research, Tokyo, Japan, 1974* (International Atomic Energy Agency, Vienna, Austria, 1975), Vol. II, p. 13.

²A. G. Dikii, Yu. K. Kuznetsov, O. S. Pavilichenko, V. K. Pashney, N. F. Perepelkin, V. A. Supruneko, and V. T. Tolok, in *Proceedings of the Fifth International Conference on the Plasma Physics and Controlled Nuclear Fusion Research, Tokyo, Japan, 1974* (International Atomic Energy Agency, Vienna, Austria,

1975), Vol. II, p. 45.

³H. Hacker, G. Pacher, H. Renner, S. Rehker, H. Ringler, and E. Würsching, in *Proceedings of the Fifth International Conference on Plasma Physics and Controlled Nuclear Fusion Research, Tokyo, Japan, 1974* (International Atomic Energy Agency, Vienna, Austria, 1975), Vol. II, p. 3.

⁴W. Stodiek, in *Proceedings of the Fifth European Conference on Controlled Fusion and Plasma Physics, Grenoble, France, 1971* (Service d'Ionique Générale, Association EURATOM-Commissariat à l'Energie Atomique, Centre d'Etudes Nucléaires de Grenoble, Grenoble, France, 1972), Vol. II, p. 1.

⁵E.g., L. A. Artsimovich, *Nucl. Fusion* **12**, 215 (1972).

⁶E.g., H. P. Furth, *Nucl. Fusion* **15**, 487 (1975).

⁷C. C. Daugheny, *Nucl. Fusion* **15**, 967 (1975).

⁸M. Murakami, J. D. Callen, and L. A. Berry, *Nucl. Fusion* **16**, 347 (1976).

⁹L. A. Berry, J. F. Clarke, and J. T. Hogan, *Phys. Rev. Lett.* **32**, 362 (1974).

Interaction of Beams of Radiation of Finite Diameters within a Plasma

E. S. Weibel*

Laboratory of Plasma Studies, Cornell University, Ithaca, New York 14850

(Received 27 September 1976)

Two beams of waves of finite diameters intersecting within a magnetized plasma emit a secondary beam of waves, provided a resonance condition is satisfied. The field of the secondary beam and the total power emitted are determined for arbitrary directions and polarizations of the incident beams. This process could be used as a means of time- and space-resolved diagnostics since it yields two relations between the density, the temperatures, and the magnetic field. Explicit formulas are given for the case of two beams in the ordinary mode producing a lower hybrid wave.

When two beams of radiation, with ω_j and \vec{k}_j , $j = 1, 2$, intersect within a plasma, they generate in the interaction volume a second-order polarization which emits a new wave, provided that $\omega_0 = \omega_2 \pm \omega_1$ and $\vec{k}_0 = \vec{k}_2 \pm \vec{k}_1$ satisfy the dispersion relation $\Delta(\omega_0, \vec{k}_0) = 0$ of this wave. In this case, power is transferred from the primary beams to the new beam according to the Manley-Rowe¹ relations

$$\delta P_1 + \delta P_2 = P_0,$$

$$\pm \frac{\delta P_1}{\omega_1} = \frac{\delta P_2}{\omega_2} = \frac{P_0}{\omega_0}$$

(assuming $\omega_2 > \omega_1 > 0$). This process can in principle be used as the basis of a new method of plasma diagnostics. In order to implement this method one of the incident beams should be frequency-modulated over a range that covers the resonance $\Delta(\omega_0, \vec{k}_0) = 0$. The emerging beams will then be amplitude-modulated, allowing syn-

chronous detection. Thus one determines ω_0 and \vec{k}_0 which satisfy $\Delta = 0$, which establishes a first relation between the density, the temperatures, and the magnetic field within the small volume defined by the intersection of the primary beams. The theory also gives explicitly the power P_0 in the form

$$P_0 = M(\mu) P_1 P_2 / P^*,$$

where $M(\mu)$ is a resonance factor, taking its maximum when the mismatch μ vanishes. Thus the measurement of the amplitude modulation (that is, of δP) of one of the emerging beams yields a second relation among the plasma parameters.

The characteristic power P^* gives a measure of the minimum power required to observe this process. Let $(\delta P_1 / P_1)_{\min}$ be the smallest detectable modulation, then one must have

$$P_2 \geq \frac{\omega_0}{\omega_1} P^* \left(\frac{\delta P_1}{P_1} \right)_{\min}.$$